

IAC-24-B2.2.4x85275

Towards comprehensive Location and Attitude Determination for a rolling, wind-driven Mars Rover

**Tim Holthuijsen^{a*}, William Moretti^a, Marcus Dyhr^a, Abhimanyu Kovithal^a, Tolga Ors^a and Julian
Rothenbucher^a**

^a*Team Tumbleweed*, * Corresponding Author, tim@teamtumbleweed.eu

Abstract

In pursuit of reliable and accurate location determination for a wind-driven Mars rover, we aim to create a comprehensive localisation system designed to meet the unique challenges of the Martian surface. The absence of conventional GNSS, combined with the Tumbleweed rover's rotating, low-cost, and low-weight design presents unprecedented challenges for Location and Attitude Determination (LAD).

To address the need of robust LAD, we are developing a fusion of sensors activated at different times of the Martian day to autonomously and reliably determine the rover's location and attitude. The total mass of the LAD payload with processors has to be less than 1kg and run on less than 5W mean power. Our LAD system is designed to operate within these strict constraints. The study begins with classifying and evaluating contemporary LAD sensors based on mass, size, and processing power, providing a basis for optimal sensor selection. The sensors are reviewed to highlight their strengths, weaknesses, and applicability to rovers with stringent requirements.

To develop, test, and demonstrate our LAD system, we have created a novel Martian environment simulation with a virtual wind-driven Tumbleweed rover. This simulation, including the rover's movement and sensor output, was made using the real-time development platform Unity. Our work includes a mechanically accurate rover model, as well as the integration of real, high-resolution Martian elevation, colour, and wind profile data to make the Martian environment as realistic as possible. Although originally developed for LAD, other Tumbleweed sub-teams can also utilise the simulation for mission planning, trajectory estimations, and for testing new mechanical structures as our rover design evolves.

This paper specifically focuses on the development of real-time, relative LAD methods to be applied during the Martian day: during daytime, the LAD algorithm utilises inertial measurement units and rotary sensors for relative location determination. At night, when solar power is unavailable and the rover's movement is halted, slower LAD methods such as star tracking, inter-rover ranging, and relay satellite localisation will be employed for absolute position determination.

Keywords: rover navigation, location and attitude determination, mars exploration, swarm, simulation

Acronyms/Abbreviations

DTM: Digital Terrain Model
GIS: Geographic Information System
HiRISE: High-Resolution Imaging Science Experiment
IAC: International Astronautical Congress
IMU: Inertial Measurement Unit
LAD: Location and Attitude Determination
MCD: Mars Climate Database
MEMS: Micro-Electro-Mechanical Systems
SCS: Stereo Camera System

increase the capacity of planetary exploration. The specific design choices made to achieve this necessitate unusually stringent requirements for the navigation sensors in terms of mass, size, cost and processing power.

This paper details how using a swarm of rovers enhances data collection efficiency and explains the critical role of a Location and Attitude Determination (LAD) algorithm in supporting scientific objectives, as well as elaborating on the challenges associated with a LAD algorithm tailored for a lightweight, rolling, low-cost Mars rover.

1. Introduction

The Tumbleweed Mission [1] consists of a swarm of autonomous, wind-driven, solar-powered, elliptical, rolling Mars rovers designed to reduce the cost and

In all known papers, classification of mass and size is subjective [2] [3]. This paper is a first attempt to use absolute values for the classification of sensors. This quantified classification is required for a LAD payload that is not to exceed 1 kg. The advantages and

disadvantages of each sensor type in terms of accuracy, mass, size and computational processing requirement are also explained and compared.

Section 2 describes the Unity simulation of the Martian environment and Tumbleweed rover, highlighting how it supports the development and validation of the LAD algorithm. This simulation was created to generate data from our simulated LAD sensors, as well as to serve as a means to test and validate the Tumbleweed rover's behaviour in a Martian environment. The section starts with a description of the model of the rover and its limitations, followed by a description of the sensor placement and the data logging. This is followed by the methodology for terrain and wind generation, and briefly touches on the simulation's user interface. Our latest version of the simulation is built based on a high-resolution Digital Terrain Model (DTM) of Mars, overlaid with a corresponding Martian colour image, meaning that our simulated Tumbleweed rover is traversing a real place on the Martian surface. For our latest edition of the simulation, we are exploring a small section of the Jezero crater, near the Perseverance's landing spot. Additionally, the simulation uses imported wind data from the Mars Climate Database (MCD), making sure that the wind data in the simulation corresponds to the correct geographical location of the terrain.

We are using Inertial Measurement Unit (IMU) sensor measurements which we feed to our IMU LAD algorithm. In order to correct the error of the IMUs over time, we have developed a stopping mechanism for the rover: since this causes the rover to cease movement, it can be used to set the current speed back to a known reference point, resetting the aggregated error, as well as enabling absolute location determination while stationary.

The analysis section of our paper discusses the simulation results, focusing on the error between the estimated and ground truth values for location and attitude. The discussion and conclusions section comments on some of the advantages and disadvantages of our simulation, as well as discussing several plans for future work.

1.1 Motivation

Mars exploration presents a range of challenges due to the harsh Martian environment, characterised by extreme temperatures, frequent dust storms, and high radiation levels. This environment requires robust spacecraft and radiation-tolerant equipment, leading to prohibitive cost and resource requirements, ultimately making scientific exploration and investigation exclusive to governments and space agencies.

The goal of New Space start-ups is to broaden access to space and make space exploration available to non-governmental stakeholders at a fraction of the

traditional cost [4]. Team Tumbleweed is aligned with this vision, and has a solution to achieve orders of magnitude lower cost scientific data collection, while enabling the direct participation of stakeholders in Martian exploration.

As presented at the IAC 2022 and 2023, the Tumbleweed Mission architecture enables exploration of the Martian surface through low-cost, wind-driven, Tumbleweed rovers [1]. The Tumbleweed concept stands out as an innovative vehicle designed to leverage Mars' abundant wind resources for propulsion. By harnessing this natural wind, the Tumbleweed significantly enhances the mobility of scientific platforms and simplifies the design of transportation vehicles. This approach has been recognized as a promising solution for the efficient and cost-effective transport of lightweight scientific payloads across long distances on Mars.

1.2 Tumbleweed Rover

The Tumbleweed rover's bio-inspired design is not a new concept, as its foundation was conceived in the 1970s. The modern design of this rolling rover concept was investigated by NASA [5]. Team Tumbleweed's rover design is similar to the Box Kite design concept, outlined in [6], however with improvements and refinements.

Each Tumbleweed rover is split into two major structural constituents: the inner structure and the outer structure. The inner structure contains the sails, solar cells/panels and payload pod(s) and the outer structure is a shell composed of multiple arcs made from a strong but flexible material, shaping and protecting the rover. This is depicted in the schematic shown in Figure 1. The rover is slightly elliptical in shape and has a nominal diameter of approximately 5 m and a total mass of 20 kg. In the current design, the inner structure is free to rotate with respect to the outer structure, and able to rotate around one main rolling axis. It is important to note that the design of the inner structure is not completed, and the current objective is to have it always upright due to the positioning of the relatively heavy main payload pod at the bottom of the inner structure. The sails provide the drag and resultant movement through the wind, and the solar cells on the sails provide the power generation. The rover can carry a pod of up to approximately 5 kg of scientific payload, which as mentioned is planned to be primarily housed at the bottom of the inner structure. These pods house the electrical systems, thermal control systems, and many of the scientific instruments. Such a pod will have a volume of 6000 cm³ or 6 standard Cube-Sat units (6U), a peak power of 20 W, and a power capacity of 100 Wh.

1.3 Advantage of using a swarm of Mars rovers

While NASA's Curiosity and Perseverance rovers have captured the world's attention with their discoveries on Mars, nearly half of all Mars missions have unfortunately ended in failure over the years [7]. A solution to increase chances of success is to send a swarm of Tumbleweed rovers to cover a large area of Mars. Using a swarm approach would ensure that, even if some of the rovers fail or get stuck, the swarm as a whole can still achieve its objectives.

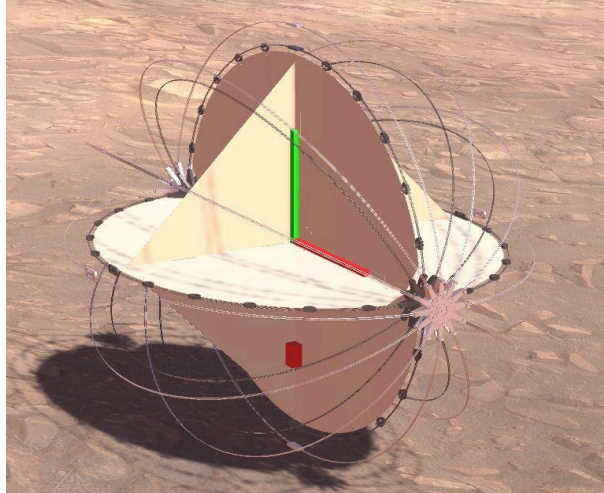


Figure 1. Latest 3D model approximation of the Tumbleweed rover.

The Tumbleweed's lightweight design in combination with their large size, flexible structure, and wind-driven locomotion allows these rovers to traverse rocky and steep terrain that has challenged wheeled rovers in the past. Tumbleweed rovers can explore inaccessible areas including canyons and craters too risky for traditional rovers. Moreover, if a Tumbleweed rover gets stuck on a geographical feature, it will simply turn into an in-situ science station, providing valuable scientific data for the rest of its stationary lifespan.

A swarm of Tumbleweed rovers could provide cheap, abundant, and sustainable locomotion on accessible planets with strong enough wind forces. The stopping mechanism will ensure that planetary protection protocols can be consistently followed. Even without wind, the Tumbleweed rovers could be dropped on mountainous regions and use the slope of the mountain and gravity to traverse down the mountain. Olympus Mons on Mars could provide a specifically interesting spot for this concept, with an elevation of 22 km that would allow a Tumbleweed to roll down a primarily downhill slope over a distance of 300 km.

1.4 Why Location and Attitude Determination?

Scientific data gathered on the surface of Mars is significantly more valuable if we are able to pinpoint exactly where this data was gathered. LAD is essential for tagging the scientific measurements in their

environment, as well as helping traverse the Martian terrain. In addition to localisation being essential for our mission design, accurate attitude determination is essential for properly operating the rover and its instruments. Many of the scientific components in our payload require the rover to be at a stable or at least a known orientation in order to function properly. As an example, the camera needs to be mostly stabilised to take proper pictures of the Martian surface. Additionally, accurately knowing the attitude of the rover at the moment a picture is taken can provide us with context on whether the landscapes and features are skewed, or if the rover's orientation is.

Put together, location and attitude determination can be used to identify the slip the rover might be experiencing, giving us information on what surface it is traversing, as well as helping us with path planning and estimation.

Naturally, the errors which are inherent to many of our sensors will affect the accuracy of our LAD algorithm, and it is our objective to keep these inaccuracies to a minimum.

1.5 Challenges and Selection of Sensors

The challenge is to find a LAD solution that has a total payload mass of less than 1 kg with low processing and power requirement.

Previous research has relied on subjective criteria for classifying sensor mass and size [2] [3]. This study presents a new approach by introducing absolute values for sensor classification. The proposed classification system is particularly relevant for space applications where the total LAD payload must remain under 1 kg.

1.5.1 Payload Size and Mass Limitation

The following classification is proposed for the sensor mass in Table 1:

Table 1. Sensor mass classifications

Mass	Classification
< 100 g	Low
100 g - 1 kg	Moderate
1-5 kg	High
> 10 kg	Very High

The following classification is proposed for sensor volume in Table 2:

Table 2. Sensor volume classifications

Volume	Classification
< 0.5U (5x5x5cm)	Small

0.5-1U	Medium
> 1U (10x10x10cm)	Large

The selected sensors are radiation hardened to withstand the conditions in space. The sensors which have been selected are the lightest available on the market with miniaturised size and low processing power requirements and the specifications are summarised in Table 3 as per the descriptions in Section 1.6.

1.5.2 Computational Load Limitations

The on-board computer and camera will primarily support scientific missions during the day, leaving minimal computational and electrical power available for LAD. To address this, the rover is planned to stop at night, when solar power is not available. Corrections to the calculated location and attitude can be made during the Martian night using star trackers, Mars satellite GNSS, Inter-Rover Ranging, and dawn/dusk sun trackers for absolute LAD to augment our daytime relative LAD. Additionally, if (computing) power is sufficiently available, visual LAD algorithms could be run to add another relative LAD sensor to fuse.

1.6 Evaluation of Suitability of Individual Sensors

1.6.1 Cameras

A potential candidate for a miniature stereo camera on the Tumbleweed mission is the Stereo Camera System (SCS), developed by UCL Mullard Space Science Laboratory. This camera was previously used on the Beagle 2 lander, which unfortunately failed to maintain communication [8]. The SCS has a mass of 360 g and occupies a volume of 520 cm³ (0.5U), making it highly suitable for missions where mass and space are limited. It operates with a mean power consumption of 1.8 W. The camera's multi-spectral capability would also allow the study of Martian rocks and regolith, including their structure, composition, mineralogy, and physical properties. Other newer cameras are also under consideration. For the Tumbleweed mission, the stereo camera is planned to be mounted on the upper side of the inner structure to ensure optimal height and maximise its field of view [9].

1.6.2 IMUs

An IMU [10] [11] is a sensor used to track an object's linear and angular acceleration through three gyroscopes and accelerometers along perpendicular axes, and will likely be one of the most important sensors in our mission design. IMUs are crucial for navigation on Earth and in space missions by providing continuous data for state estimation, although sensor drift and noise aggregation requires occasional recalibration with other tools. A miniaturised Micro-Electro-Mechanical Systems (MEMS)-based

IMU developed for space exploration is highly suitable for Mars rovers due to its compact size (weighing under 200 g), low power consumption (less than 1 W), and ability to operate in harsh Martian conditions, including extreme temperatures (-135°C to 70°C), low pressure (0 to 7 mbar), and exposure to radiation.

The IMU offers localization accuracy better than 2% and is designed for long-term missions, such as the 180-sol ExoMars mission, making it ideal for precise and reliable rover navigation on Mars. However, integrating the IMU with other systems is essential to counteract drift over long distances [12]

Most IMU's include a gyroscope, which is an instrument used to measure or maintain orientation and angular velocity. It operates based on the principles of angular momentum, where a spinning rotor or disk resists changes in its axis of rotation, making it highly sensitive to any tilting or turning motion. Modern gyroscopes, especially those used in space applications like in the Mars rover, are often based on MEMS technology, which miniaturise the device using tiny sensors to detect angular velocity. Additionally, their performance in terms of bias stability and angular random walk makes them ideal for tasks like dead reckoning and short-distance navigation on the Martian surface, contributing to the rover's ability to traverse challenging terrain [13].

1.6.3 Optical Encoders

An optical encoder [14] is a device used to convert angular or linear motion into an electrical signal for motion control applications. It works by shining a light source, typically an LED, through a coded scale or disk that has alternating transparent and opaque segments. As the disk rotates, the light passing through the transparent segments is detected by a photodiode array, generating electrical pulses. These pulses are then processed to determine the position, speed, and direction of movement. Optical encoders are commonly used in robotics, industrial equipment, and aerospace systems for precise position feedback. Optical encoders demonstrate significant potential for use in space applications like the Mars rover due to their high precision and reliability. Encoders can offer micro-radian resolution (< 0.5 μrad) and can tolerate extreme environmental conditions such as wide temperature ranges (-35°C to +75°C), low pressure, and radiation, which are similar to those encountered on Mars. Its durability over a 15-year lifetime, vibration resistance (up to 24.7 g), and low power consumption (< 3 W) make it particularly suitable for long-term missions in harsh environments. The encoder's robustness against signal degradation and its ability to maintain performance despite misalignments and contamination further enhance its reliability for Mars exploration, where conditions are challenging [15].

1.6.4 Star Trackers

A star tracker [16] is a navigational tool used to determine a spacecraft's or rover's orientation by capturing images of stars and comparing them with an onboard star catalogue. It works by detecting the positions of stars within its field of view and matching these against known celestial coordinates to calculate the orientation of the rover or spacecraft in three-dimensional space. These sensors are typically used in environments where high-accuracy attitude and absolute location determination is needed, as they offer robust performance in the absence of a magnetic field or other external references. However, challenges such as harsh environmental conditions, high cost, and reliance on clear skies might limit their effectiveness during dust storms or other Martian weather events.

1.6.5 Sun Sensors

A sun sensor [17] is a device used to determine a rover's orientation by measuring the sun's position relative to the vehicle and comparing it with precise information about the sun's location at any given time to estimate heading and, in some cases, global position. Combined with an inclinometer and clock, the sun sensor provides accurate heading data by transforming the measured sun vector into a topocentric reference frame. Tested in Mars-analog environments like Devon Island, the sun sensor system demonstrated heading accuracy within a few degrees, which is adequate for rover navigation on Mars, where magnetic compasses are ineffective due to the lack of a strong magnetic field. While sun sensors perform well under clear skies, atmospheric conditions such as dust storms could affect their reliability [18]. Nonetheless, integrating sun sensors helps counter drift of relative navigation systems, making them highly suitable for Mars exploration.

Table 3. Comparative analysis of sensor types.

Sensor Type	Accuracy	Computational Load	Volume	Power Usage	Mass
Camera	High	Moderate to High	Low	1.8 W	Moderate
IMU	Moderate	Low	Low	0.2 W	Low
Optical Encoder	Moderate	Moderate	Medium	< 3 W	Moderate
Star Tracker	Moderate	Moderate	Low	0.5 W	Low
Sun Sensor	Moderate	Moderate	Low	0.0116 W	Low

2. Simulation Model & Methodology

A 3D simulation was created in Unity primarily to generate data from simulated sensors, but also to serve as a means to test and validate the Tumbleweed rover's

behaviour in a Mars-like environment. Unity, being a real-time development platform with its own physics engine, is an effective tool to simulate sensors typically found on a planetary rover, such as rotary encoders, accelerometers, gyroscopes, cameras, star sensors, etc.

The simulation terrain was generated using a High-Resolution Imaging Science Experiment (HiRISE) DTM of the Jezero crater [19] [20] [21]. The Jezero crater location was selected as it is one of the most recent sites from which high-resolution surface data and images are available. As the Tumbleweed rover is wind-driven and doesn't have any means of self-propulsion, simulating wind as reliably as possible is of high importance. For this reason, the MCD [22] was used to get static surface horizontal wind speed data for given terrain coordinates.

2.1 Rover Model

The Tumbleweed rover's design is a dynamic process that is actively ongoing in parallel to the work on the simulation. For this reason, the rover model used in the simulation is a simplification of the expected design. The main components represented are the outer structure, the inner structure, the pods, and several virtual sensors, as seen in Figure 1. The outer and inner structures are linked together via a virtual hinge joint, allowing rotation only on the longitudinal axis. Apart from the virtual sensors, each of the components, the outer structure, inner structure, and payload pod, have been assigned a mass, respectively 5 kg, 5 kg, and 10 kg. The majority of the mass is in the pods, located at an offset from the centre of the rover, and serves to keep the inner structure in balance while the outer structure is rolling.

To adhere to planetary protection protocols and to allow for stable science observations, the rover will have the ability to stop moving via a physical mechanism. The current stopping mechanism design will lock the rotational axis between the two structures. This will require the rolling rover to lift the off-centred mass, which will decrease its speed over time and eventually come to a stop. The locking process is meant to be reversible and repeatable, allowing for some amount of control in the rover's movement. This stopping mechanism has been included in the simulation, which allows us to test and validate its effectiveness. Triggering the stopping mechanism is done manually by a user via a button on the simulation's user interface, or through planning a stop in the simulation's user interface.

2.2 Sensor Placement

Currently there are three main virtual sensors: an IMU, a camera and an optical wheel encoder. As mentioned previously, there is an ongoing design process of the rover model and the camera may not be

used for LAD. The virtual sensors have been placed at the centre of the inner structure. The wheel encoder will likely be placed at the interface between the outer and inner structure to measure the relative change in rotation between the two. For the IMU, ideally the placement is close to the centre of the inner structure. In the simulation, it has been assumed that it is at the centre of the inner structure. This placement is not the final placement, however placing it at the centre simplifies the data processing by eliminating any translational motion due to rotation of the inner structure. As the design progresses, the placement may change, as well as adding more sensors for redundancy

2.3 Data Logging

There is no precise model of the magnetic field of Mars like on Earth, therefore the magnetometer that is usually an integral part of an IMU cannot be used for location and attitude determination. As such, the virtual IMU is assumed to be a 6-DoF IMU consisting of a 3-axis gyroscope and a 3-axis accelerometer. The virtual IMU logs these data points by sampling the true attitude and acceleration of the inner structure and adds a user-defined random noise value. The noise is implemented by adding a random sample from a zero-mean standard distribution with standard deviation derived from specifications of the real sensors referenced in Table 3. The reference sensor for the IMU is the VN-100 [10], whose standard deviation of the accelerometer and gyroscope has been set to the product of its noise density and bandwidth.

There are many types of wheel encoders, however they all output a parameter that can be converted to a rotational state, be it the angular velocity or the angular position. The virtual wheel encoder in this simulation outputs the cumulative change in angular position of the outer structure with an added noise value. The reference sensor for the rotary encoder is the VLS-60. As its accuracy has been listed by the supplier at ± 0.010 degrees, the implemented noise is a random sample from a uniform distribution with range $[-0.010, 0.010]$.

Common to both virtual sensors is a sampling frequency for data logging set to 50 Hz. It is important to note that the sampling frequency is purely for data logging purposes, as all measurements are sampled from the true values of the system, whose physics are performed at a rate of 50Hz. Any sampling rate higher than this, which is what the true sample rates of the sensors would be, would result in the same measurement. Since increasing the sampling frequency would increase the overall simulation's framerate, and thus the processing power required, a compromise was made to ensure consistent data logging. This is one of the limitations of using Unity as the simulation tool, which is not purpose-built for this type of simulation.

In addition to the data logged by the virtual sensors, the ground truths for all relevant parameters in the simulation have also been logged for comparison purposes in the data analysis.

2.4 Terrain Generation

The process of generating a 3D terrain from a HiRISE DTM [19] [20] was done in three steps: (a) Import and process the DTM in a GIS software, (b) rescale and convert the GIS-processed file into 16-bit RAW format, and (c) generate the terrain in Unity.

(a) As a DTM contains geo-referenced elevation data, a Geographic Information System (GIS) must be used to process that data. For this, the QGIS software was selected, as it is open-source. The data processing required is dictated by Unity's terrain tool, which expects a height map image with a resolution size in pixels equal to a power of two. Therefore, a new geo-referenced image in TIFF format was extracted in QGIS based on a set area of 2 km by 2 km and was selected for its flatness with a maximum elevation of 62.1 m. The resulting greyscale elevation image is shown in Figure 2. Using the same method, a coloured image of the same location was also processed to be used as the base colour texture of the final generated terrain.

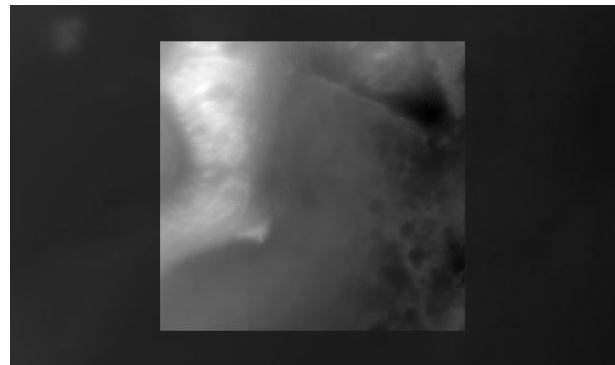


Figure 2. Extracted elevation data, representing a 2 km by 2 km area in the Jezero crater with a maximum elevation of 62.1 m, centred at 77.436 N, 18.421 E.

(b) Given the extracted 32-bit TIFF image of the previous step, a rescaling and a conversion are required to produce a new image file with the 16-bit RAW image format expected by Unity. Both treatments were performed using Python. At the same time, the Python script is used to display to the user the necessary parameters for the last step, as seen in Table 4.

Table 4. Parameters of the extracted terrain area.

Coordinate system	Equirectangular Mars 2000 Sphere IAU
Resolution (m/px)	0.5

Size (m)	2048 x 2048
Relative elevation (m)	62.071
Latitude range	77.4192 N – 77.4538 N
Longitude range	18.4042 E – 18.4388 E

(c) Unity’s Terrain Toolbox package was used for the generation of the 3D terrain. The created object is a 3D surface following the elevation data, configured to allow for other objects to physically interact with the terrain. In addition to the terrain’s RAW image, its dimensions and its height, textures were added to give the surface a Martian look.

2.5 Wind Simulation

As mentioned previously, wind is an important factor of the simulation, as it is one of the main forces acting on the rover. Even though a global wind speed value could have been used, the approach of using a 2D grid was preferred, where each grid cell represents a different wind speed value. In the current state of the simulation, the wind grid is made of 441 (21x21) identical cells and covers the entire terrain.

Calculated wind speeds on Mars are available from the MCD. Given a set of inputs, such as latitude, longitude, altitude, climatology scenario, and more, the MCD outputs geo-referenced climate data, including horizontal wind speed vectors. Each horizontal wind speed vector consists of a West-East component and a South-North component. A Python script was created to produce a two-dimensional table of horizontal wind speed vectors, based on the range of latitudes and longitudes of the generated terrain, and at an altitude of 1 m above the surface. This wind data file was then used in Unity to assign a wind vector to each of the wind grid cells. A section of the wind grid is illustrated in Figure 3. Finally, calculating the force of the wind acting on the rover was done using Equation 1.

$$F_w = \frac{1}{2} C_d \rho v^2 A$$

Equation 1. Wind load on a surface, where:

F_w = wind force (N)

C_d = aerodynamic drag coefficient

ρ = air density on Mars (kg/m^3)

v = horizontal wind speed (m/s)

A = rover’s sails cross-sectional surface area (m^2)

While the simulation is running, the wind force in action is taken from the wind grid cell in which the rover is located. As it currently stands, the aforementioned wind implementation in the simulation is static and doesn’t account for variability over time or wind gusts. Fixed values for the air density and for the sails surface have been used in the calculation,

respectively of $0.02 \text{ kg}/\text{m}^3$ and 15.904 m^2 (2.25 m radius). Based on results from wind tunnel measurements using a similar vehicle design [23], an aerodynamic drag coefficient value of 0.75 was used. Given the complex and unpredictable nature of the wind, improvements will have to be made and are discussed in Section 5. The main reason for using a grid was to make it relatively easy to add the influence of other factors, such as wind speed variation, across the span of the terrain, while keeping the computational load to a minimum.

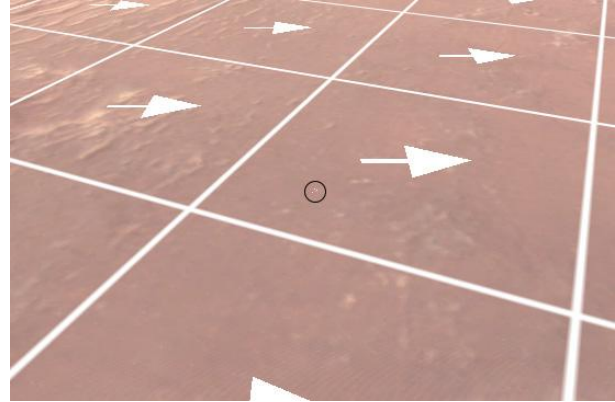


Figure 3. Tumbleweed rover (encircled) in a virtual grid of vectors representing the wind speed at that location.

2.6 User Interface

The simulation’s user interface consists of several panels. The top panel includes the controls used to load a parameter file, as well as play, pause, reset and quit the simulation. An option is also present to trigger a pause after a set amount of time. The top left panel shows several display options and initial parameters, such as gravity and rover location, rotation and altitude. The bottom left panel shows various live statistics, such as the time elapsed, the rover speed, the distance travelled, etc. Those statistics are updated once every frame. The right panel lists buttons to issue commands to the rover. Currently, only commands to trigger and release the rover’s stopping mechanism are available. Figure 4 shows the simulation’s user interface.

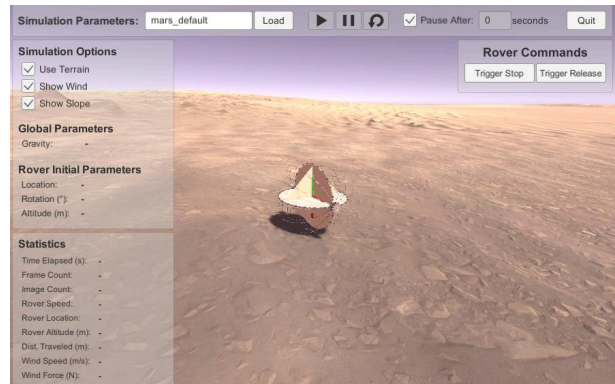


Figure 4. The simulation's user interface, showing the simulation controls at the top, initial and live parameters on the left, as well as rover commands on the right.

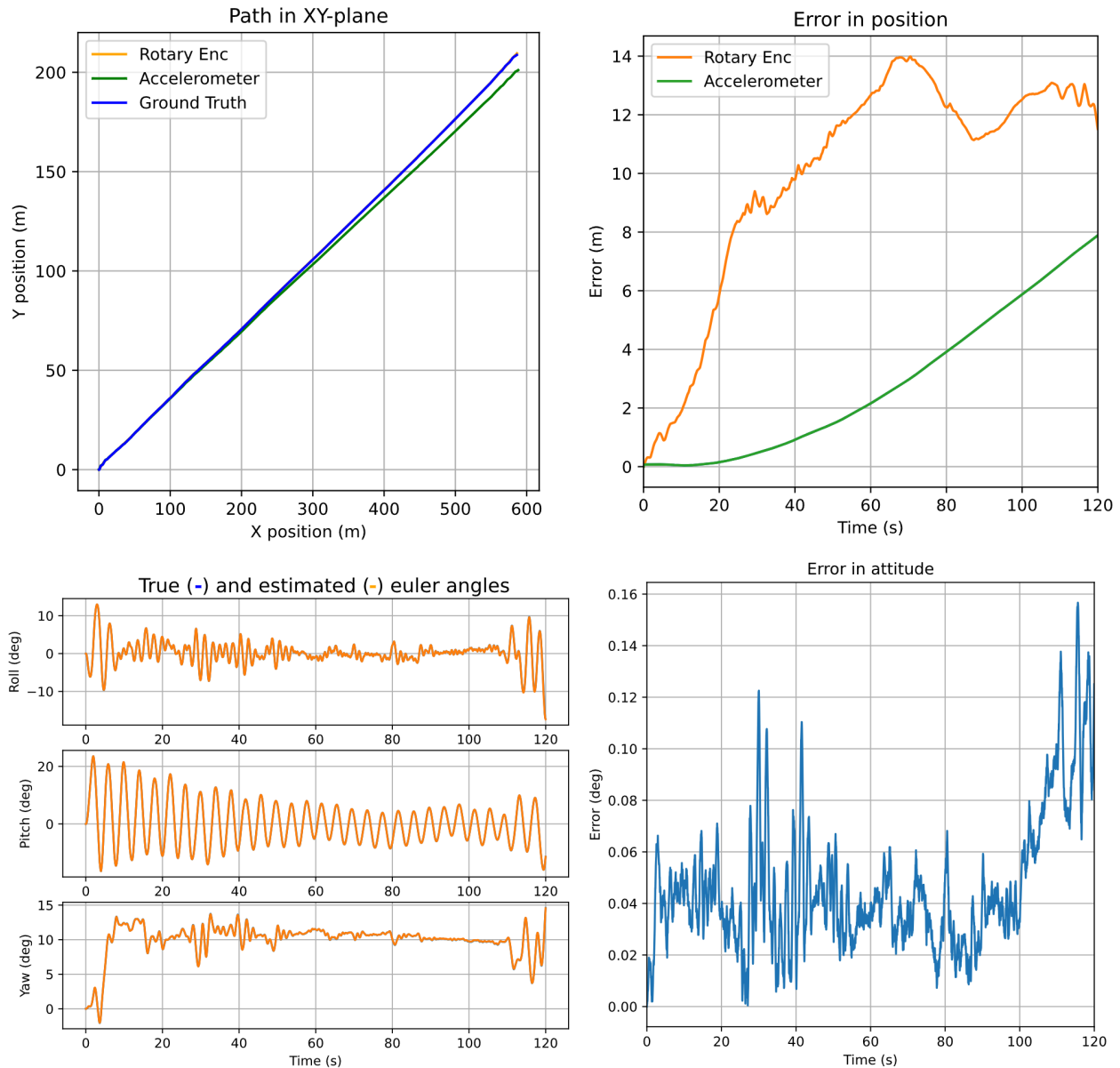


Figure 5. Location and Attitude graphs showing path, attitude and error over time. (a) *Top-left*: The ground truth of the path in the XY-plane taken by the Tumbleweed rover during simulation has been plotted in blue, with estimations of the true path by the accelerometer and rotary encoder in green and orange respectively. Due to near-perfect overlap, the green and orange lines are hidden behind the blue line. (b) *Top-right*: The error propagation over time has been plotted in green for the accelerometer and orange for the rotary encoder. (c) *Bottom-left*: The ground truth in blue of the euler angles of the inner structure together with the estimation from the gyroscope in orange. Blue line hidden due to overlap. (d) *Bottom-right*: The error as a function of time has been plotted for the euler angles, with error being the distance in degrees between true and estimated euler angles.

3. Analysis of Simulation Output

3.1 Data Processing

The data gathered by the emulated sensors during the simulation has been processed to give an estimate of

location and attitude. The analysis based on this data is meant to provide insight into the current progress of the location and attitude determination. As a start to future more complex algorithm designs, the simple approach of dead reckoning has been tested. Dead reckoning is a double integral of the measured linear acceleration or single integral of the measured angular velocity, which outputs the linear or angular position over time respectively. In practice however, the angular positions are found by iteratively using the angular velocities to estimate a quaternion representing the change in attitude at that moment of time, which then updates the attitude. Hereby we get the attitude as a function of time.

The rotary encoder was used to measure the cumulative amount of rotation of the outer structure in the pitch axis, which is the axis the Tumbleweed rolls around. This rotation was converted to a distance by multiplying the cumulative amount of degrees by the circumference of the rover and dividing by 360 degrees. Together with the angular positions from the gyroscope, the distance covered at each time step was then computed to estimate the path the rover covered.

3.2 Data Visualisation & Analysis

The true attitude of the inner structure and the attitude derived from the measured angular velocities have been plotted on Figure 5-c as Euler angles. The estimated values in orange seem to almost completely overlap the ground truth in blue for all three Euler angles. This indicates that the attitude of the system can be quite accurately determined. However, measurements from a real gyroscope usually include very high frequency noise, which is largely absent in both the ground truth and estimated values. This is likely due to the 50 Hz sampling frequency limitation mentioned in Section 2.3. This limitation may contribute to the similarity between the two curves. Additionally, the total runtime of the simulation was only 120.0 seconds for the plots shown in the analysis section—a relatively short time compared to the actual duration the rover will need to accurately estimate its attitude. As shown in the error plot (Figure 5-d), the total error increases over time, which could result in poor performance over longer timescales if absolute LAD is absent.

The true path the rover took and the estimated path using the accelerometer and the rotary encoder has been plotted in Figure 5-a in blue, green and orange, respectively. Similar to the Euler angles, the estimated paths and the true path seem to overlap greatly indicating a good estimation of location throughout the simulation runtime. However, when a closer look is taken at the error between the ground truth and the estimations as on Figure 5-b we see that the error steadily increases over time. The error plotted is the distance in (x,y,z) between the ground truth and the estimations, so it accounts for more than just the

XY-plane that is shown on Figure 5-a. If the tendency from the limited runtime continues as it is, then one could expect large discrepancies between the ground truth and the estimated position for the real rover with this current implementation.

4. Results

The error between the ground truth and the estimated location and attitude seems to increase over time. This tendency is to be expected as dead reckoning which relies on integration of noisy measurements will continue to accumulate error. The total error at the end of the simulation was 7.89 m and 11.52 m for the accelerometer and rotary encoder respectively. As these errors are expected to increase over time, a better LAD system with appropriate noise filtering should be put in place to ensure that an accurate estimate of location is kept. With the stopping mechanism, the accumulated location error could, in theory, be counteracted if another method, such as inter-rover ranging or satellite navigation signals, reliably provides absolute location determination. The IMU could then be used to track relative location changes between these estimated absolute positions.

Although the accumulated error of the attitude is below 0.2 degree during simulation runtime, for real gyroscopes with more realistic noise at higher frequencies it is to be expected that more advanced techniques would be necessary. For the determination of attitude, more commonly used techniques such as sensor fusion with simple filters such as a complementary filter or more industry-standard filters like an Extended Kalman filter or Madgwick filter would be fitting.

5. Discussion & Conclusions

The rover model used in the simulation is a simplified version, as the final design is not completed yet. In fact, it is important to conduct simulation testing in parallel to mechanical design, as the results of the simulation can potentially be used to inform the design. In other words, several design assumptions were made in the rover model, and will likely change in the future. One such assumption is the mechanics of the inner structure as its design is still in a premature state. Nevertheless, it is a crucial component of the simulation, as it contains all sensors and is necessary for them to be stabilised relative to the horizon.

The current method of generating a Martian-like 3D terrain was used to add realism to the simulation, however it has some disadvantages. Relying on publicly available DTMs limits the amount of surface details, specifically elevation resolution. In addition, Unity imposes restrictions on image dimension and terrain resolution. While it would be possible to develop a

custom terrain generation tool, the need for such a solution was not encountered in the present study. Another disadvantage of using a fixed-size terrain is the lack of horizon from the perspective of the rover. As such, horizon detection wouldn't be possible if a visual odometry algorithm is added in the future. The main underlying issue is that adding more terrain has a significant computing cost in Unity, which may impact the data logging process.

In terms of wind simulation, it has already been mentioned that a simplified approach is currently being used. Given the very low atmospheric density on the Martian surface, the resulting wind force is small compared to a force from an equivalent wind speed on the surface of Earth. In the current state of the simulation, this means it is likely that the Tumbleweed rover will start to roll backwards in the presence of an uphill terrain, which could eventually lead to the rover being trapped in a local minimum. As wind is a key factor for a wind-driven rover, future work will have a strong focus on improving simulated wind behaviour and its interaction with the rover. One such improvement would be to include perturbations in the winds speeds extracted from the MCD, as well as to include air density variability, wind speed change over time, and the addition of high-speed gusts. Since drag defines movement of the rover, it will be critical to refine our model and determine the most accurate wind and surface drag coefficients possible.

The next clear step in terms of sensors would be to implement and test more sensors capable of providing location and attitude estimations. A rolling Tumbleweed rover provides interesting challenges within fields such as visual odometry, which may be an interesting addition to our LAD algorithm. Incorporating additional sensors would enable the implementation of sensor fusion algorithms, such as the Extended Kalman Filter or Madgwick Filter, thereby enhancing the accuracy of these estimations. With a more advanced location and attitude determination scheme it may soon be possible to start comparing performance not just between different sensors but between different rover designs, thereby aiding the ongoing engineering development of the Tumbleweed rover and similar future rovers.

There is a lot of activity with regards to providing navigation assistance to rovers on Mars. Existing Mars relay satellites can transmit positioning signals [24] [25], aiding in the absolute location determination and reducing location errors overnight when the rover is stationary. Additionally, star sensors provide an effective method for resetting accumulated errors in attitude during these periods of inactivity [18].

The simulation results show promising performance for the LAD system of the Tumbleweed rover, but also highlight areas for improvement. Over a relatively short simulation runtime of 120.0 seconds, the attitude

estimation using the gyroscope data closely matched the ground truth, with errors below 0.2 degrees. However, the location estimation, while initially accurate, showed a steady increase in error over time. By the end of the simulation, the accelerometer-based estimation had an error of 7.89 metres, while the rotary encoder-based estimation had an error of 11.52 metres.

A critical finding emerged when using real Martian wind and elevation data: the rover could become stuck due to insufficient wind force, especially in areas with uphill terrain. This highlights the paramount importance of carefully selecting the initial dropping location for the rover and accurately simulating Martian winds. The low atmospheric density on Mars results in relatively weak wind forces, which may be inadequate to propel the rover during periods of low wind speed.

This discovery again underscores the need for extensive pre-mission analysis and simulation of potential landing sites considering the Mars topography and prevailing wind patterns, thus paving the way for the most optimized and effective Mars mission possible.

References

- [1] L. Cohen. *et al.*, Pre-Phase A study of an innovative, low-cost Demonstration Mission of Tumbleweed mobile impactors on Mars, 74th International Astronautical Congress (IAC), Baku, Azerbaijan, 2023
- [2] Y. Cai, T. Qin, Y. Ou, and R. Wei, Intelligent Systems in Motion: A Comprehensive Review on Multi-Sensor Fusion and Information Processing From Sensing to Navigation in Path Planning, International Journal on Semantic Web and Information Systems, Vol. 19 Issue 1, 2023.
- [3] M.O.A. Aqel, M.H. Marhaban, M.I. Saripan, and N.Bt. Ismail, Review of visual odometry: types, approaches, challenges, and applications. SpringerPlus 5, 1897 (2016). doi: [10.1186/s40064-016-3573-7](https://doi.org/10.1186/s40064-016-3573-7)
- [4] A. Golkar and A. Salado, Definition of New Space—Expert Survey Results and Key Technology Trends, IEEE Journal on Minitiarization for Air and Space Systems, VOL. 2, NO. 1, March 2021.
- [5] J. Antol *et al.*, Low cost mars surface exploration: the mars tumbleweed. National Aeronautics and Space Administration, Langley Research Center, 2003.
- [6] G. Hajos, J. Jones, A. Behar, and M. Dodd, An overview of wind-driven rovers for planetary exploration, in 43rd AIAA Aerospace Sciences Meeting and Exhibit, 2005, p. 244.

- [7] M.K. Biswal and R.N. Annavarapu, Mars Missions Failure Report Assortment: Review and Conspectus, AIAA Conference on Propulsion and Energy, August 2020.
- [8] A. Griffiths *et al.*, “The beagle 2 stereo camera system,” Planetary and Space Science, vol. 53, no. 14-15, 2005, pp. 1466–1482.
- [9] D. Tjokrosetio *et al.*, Identification of Human Landing Sites on Mars with a Swarm of Wind-Driven Mobile Impactors, 74th International Astronautical Congress (IAC), Baku, Azerbaijan, 2023.
- [10] VectorNav VN-100 IMU product information. <https://www.vectornav.com/products/detail/vn-100>, Accessed September 2024.
- [11] Safran STIM300-IMU product information. <https://www.sensor.com/products/inertial-measurement-units/stim300>, Accessed September 2024.
- [12] F. Rehrmann, J. Schwendner, J. Cornforth, D. Durrant, A Miniaturised Space Qualified MEMS IMU for Rover Navigation - Requirements and Testing of a Proof of Concept Hardware Demonstrator, 11th ESA Workshop on Advanced Space Technologies for Robotics and Automation, April 2011. doi: <https://www.researchgate.net/publication/277331920>
- [13] Y. Zhuang *et al.*, Multi-sensor integrated navigation/positioning systems using data fusion: From analytics-based to learning-based approaches. Information Fusion. Vol. 95, 2023, pp 62-90, doi: [10.1016/j.inffus.2023.01.025](https://doi.org/10.1016/j.inffus.2023.01.025).
- [14] Netzer VLS-60 Rotary encoder information. <https://netzerprecision.com/products/vls-60/>, Accessed September 2024.
- [15] M. Reinhardt, K Panzlaff, K Friederich, F. Heine, “High Precision Encoders for GEO Space Applications,” International Conference on Space Optical Systems and Applications, Corsica, France, Oct. 2012.
- [16] Twinkle Star Tracker product information. <https://www.arcsec.space/twinkle/>, Accessed September 2024.
- [17] GomSpace NanoSense Fine Sun Sensor for High Precision ADCS Control product information. [https://gomspace.com/shop/subsystems/attitude-orbit-control-systems/nanosense-fss-\(1\).aspx](https://gomspace.com/shop/subsystems/attitude-orbit-control-systems/nanosense-fss-(1).aspx), Accessed September 2024.
- [18] J. Enright, P. Furgale and T. Barfoot, Sun sensing for planetary rover navigation, IEEE Aerospace conference, April 2009, pp. 1-12. doi: [10.1109/AERO.2009.4839311](https://doi.org/10.1109/AERO.2009.4839311).
- [19] Y. Tao, S. H. G. Walter, and J.-P. Muller, “Refinement of the Mars 2020 Terrain Relative Navigation HiRISE DTM Mosaic using Deep Learning.” Freie Universität Berlin, 2023. doi: [10.17169/refubium-38359](https://doi.org/10.17169/refubium-38359).
- [20] A. S. McEwen *et al.*, “Mars Reconnaissance Orbiter’s High Resolution Imaging Science Experiment (HiRISE),” *J. Geophys. Res.*, vol. 112, no. E5, May 2007. doi: [10.1029/2005JE002605](https://doi.org/10.1029/2005JE002605).
- [21] R. L. Fergason, D. M. Galuszka, T. M. Hare, D. P. Mayer, and B. L. Redding, “Mars 2020 Terrain Relative Navigation HiRISE DTM Mosaic.” U.S. Geological Survey, 2020. doi: [10.5066/P9REJ9JN](https://doi.org/10.5066/P9REJ9JN).
- [22] E. Millour, Mars Climate Database, <https://www-mars.lmd.jussieu.fr/mars/access.html>, Accessed September 2024.
- [23] S.E. Rose, C.B. Moody, D.L. James, A.A. Barhorst, “Drag measurement and dynamic simulation of Martian wind-driven sensor platform concepts.” Journal of Fluids and Structures, vol. 22, no. 1, 2006, pp. 21-43. doi: [10.1016/j.jfluidstructs.2005.09.008](https://doi.org/10.1016/j.jfluidstructs.2005.09.008).
- [24] J. Taylor, D. K. Lee, and S. Shambayati, Mars Reconnaissance Orbiter, 29 July 2016. https://descanso.jpl.nasa.gov/monograph/series13/DeepCommo_Chapter6--141029.pdf
- [25] X. Xiong, H. Wang and Q. Zhou, "Autonomous navigation of the Mars approach based orbiters radiometric measurement," 2022 41st Chinese Control Conference (CCC), Hefei, China, 2022, pp. 3468-3473. doi: [10.23919/CCC55666.2022.9902151](https://doi.org/10.23919/CCC55666.2022.9902151).